engineering proceedings

MDPI

Proceeding Paper

Time-Dependent Adaptations of Brain Networks in Driving Fatigue †

Olympia Giannakopoulou [1,*], Ioannis Kakkos [1,2], Georgios N. Dimitrakopoulos [3], Yu Sun [4], George K. Matsopoulos [1] and Dimitrios D. Koutsouris [1]

[1] Biomedical Engineering Laboratory, National Technical University of Athens, 15772 Athens, Greece; ikakkos@biomed.ntua.gr (I.K.); gmatsopoulos@biomed.ntua.gr (G.K.M.); dkoutsou@biomed.ntua.gr (D.D.K.)
[2] Department of Biomedical Engineering, University of West Attica, 12243 Athens, Greece
[3] Department of Informatics, Ionian University, 49100 Corfu, Greece; geo.dimitrakopoulos@gmail.com
[4] Key Laboratory for Biomedical Engineering of Ministry of Education of China, Department of Biomedical Engineering, Zhejiang University, Hangzhou 310027, China; yusun@zju.edu.cn
* Correspondence: ogiannakopoulou@biomed.ntua.gr
† Presented at the Advances in Biomedical Sciences, Engineering and Technology (ABSET) Conference, Athens, Greece, 10–11 June 2023.

Abstract: Driving with fatigue is a major contributor to traffic accidents and is closely linked to central nervous system functions. To investigate the evolution of brain dynamics during simulated driving under different EEG rhythms, we conducted an experiment in which participants performed a 1 h driving task while their EEG signals were recorded. We used the complex network theory to analyze data derived from the driving stimulation and found that as fatigue deepened, small-world metrics, namely the path lengths, clustering coefficients, and measures of efficiency (global, local, nodal), showed alterations against the driving time. Additionally, a major correlation (corr = 0.98) was observed between the cluster coefficient with local efficiency in all frequency bands (theta, alpha, beta). Our findings suggest that driving fatigue can cause significant trends in brain network characteristics, such as path length (m = −103 to −93), (m = 98) for specific rhythms (beta, alpha, theta band, respectively) and their related brain functions, which could serve as objective indicators when evaluating the fatigue level and in the future, preventing driving fatigue and its consequences.

Keywords: EEG; PLI networks; driving fatigue; small-world metrics; functional connectivity

Citation: Giannakopoulou, O.; Kakkos, I.; Dimitrakopoulos, G.N.; Sun, Y.; Matsopoulos, G.K.; Koutsouris, D.D. Time-Dependent Adaptations of Brain Networks in Driving Fatigue. *Eng. Proc.* **2023**, *50*, 6. https://doi.org/10.3390/engproc2023050006

Academic Editors: Dimitrios Glotsos, Spiros Kostopoulos, Emmanouil Athanasiadis, Efstratios David and Panagiotis Liaparinos

Published: 31 October 2023

1. Introduction

According to WHO (World Health Organization), car accidents were responsible for 1.35 million deaths worldwide in 2016 [1]. As a result, effective assessments of mental workload, fatigue, and drowsiness are crucial to capitalize on road safety and reduce traffic-related accidents. In fact, it is commonly believed that drowsiness in drivers is a highly important factor concerning car accidents [2]. Mental fatigue is a psychobiological state caused by long periods of demanding cognitive performance and affects many everyday activities, such as safe driving capabilities [3]. It is linked with deteriorated performance, which can be subjectively assessed via behavioral characteristics, such as escalated reaction times and increased errors.

To assess the properties of mental fatigue, the detection of alterations in the brain is widely proposed as a more objective evaluation estimator, revealing strong indications of fatigue levels [4]. However, the detection of fatigue-related effects in real-world environments is a current challenge and requires a deeper investigation into the neural mechanisms associated with mental fatigue. Recent studies on brain functional connectivity analysis have been promising for the enrichment of existing knowledge. Moreover, the application of the graph theory in neuroscience has provided a valuable approach for quantitatively evaluating brain reorganization as a result of mental fatigue [5,6].

In this regard, different approaches and methods for the construction of functional networks have been proposed and utilized (such as partial-directed coherence, the direct transfer function, or phase lag index (PLI)) [7,8] representing statistical dependence and a directed information flow between cortical regions, as well as an analysis of intrinsic brain network mechanisms. Many recent studies on electroencephalography (EEG) have focused on modeling and estimating brain connectivity due to increasing evidence that it can help better understand various brain neurological conditions [9]. While recent advances in the development of quantitative EEG analysis methods have allowed for the investigation of interactions across the cerebral cortex during fatigue and neural markers of cognitive fatigue have been identified [10], there are still some significant limitations; group-level statistical methods do not provide a mechanism to predict the state of mental fatigue based on the functional connectivity network at the individual level [11,12].

In this paper, we applied PLI functional connectivity on EEG data derived from a driving experiment specially designed to induce fatigue. The created networks were analyzed in terms of functional brain reorganization. Our results display fatigue-related trends in several small-world metrics, suggesting distinct indicators of cognitive exhaustion.

2. Materials and Methods

2.1. Participants and Experimental Design

The present study recruited a total of 20 right-handed students and staff members (age = 23.4 ± 5.4 years) from the National University of Singapore (NUS). All participants had valid driving licenses and normal or corrected-to-normal vision. The simulated driving task was performed using City Car Driving (Version 1.5, http://citycardriving.com/ (accessed on 26 May 2023)) with left driving rules according to Singapore standards and utilizing the driving wheel, pedals, and gearbox equipment (Logitech G27 Racing Wheel, Logitech International SA, Lausanne, Switzerland). Based on the results of previous driving fatigue studies, the duration of the task was set at 1 h for salient fatigue-inducing effects. Electroencephalogram (EEG) data were captured utilizing 64 scalp electrodes made of an Ag/AgCl material, following the conventional 10–20 system (manufactured by Waveguard, ANT B.V., Hengelo, Netherlands) and sampled at a rate of 512 Hz. The unprocessed EEG signals underwent band-pass filtering within the frequency range of 1 to 40 Hz. These signals were then re-referenced to the mean of the electrodes positioned on both the left and right mastoid areas and were subsequently reduced in the sampling rate to 256 Hz. The route included a motorway and a rural road, containing mainly a straight road with a minimum level of traffic in order to make the task less demanding and, therefore, subjects more prone to drowsiness [11].

2.2. Functional Connectivity and Brain Network Construction

The phase lag index (PLI) was used to calculate functional connectivity between all pairs of 64 electrodes for each frequency band and segment separately. In general, the PLI is an estimation of phase synchronization that is targeted to minimize the effects of volume conduction in EEG signals by disregarding zero and π phase differences (angles). The PLI quantifies the asymmetry of the distribution of instantaneous phase differences, which are set using the Hilbert transformation [13]. A distribution that is symmetric and centered around zero could indicate spurious connectivity, and a flat distribution indicates no connectivity. Deviances from a symmetric distribution represent dependency between sources. The PLI can be obtained from the time series of phase differences $\Delta\varphi\,(t_k)$, k = 1. . .N by means of the following:

$$PLI = |\langle \sin[\Delta\varphi(tk)] \rangle| \quad (1)$$

The PLI values range between 0 and 1. A zero value means no coupling or coupling with a phase difference centered about zero. A value of 1 indicates exact phase locking at a non-zero value of Δφ. PLI values close to 1 suggest strong non-zero phase locking [13].

The statistical significance of PLI values was estimated using an empirical distribution from 100 surrogate networks at the 5% threshold. For connectivity estimation, driving data were divided in a continuous fashion into windows of 5 min with a 50% overlap. Finally, one average PLI network (62 × 62 weighted directed adjacency matrix) was obtained from each participant.

2.3. Network Analysis

Before network analysis, the same sparsity value was used for all the networks in order to compare topological graph measures, preventing any bias originating from different edge numbers [14]. The property of sparsity [15] in a network and the current context is defined as the ratio of the number of present edges to the number of all possible edges in a fully connected network. Several levels of network sparsity were applied, ranging from 0.1 to 0.3, with a step of 0.05 and a common sparsity s = 0.25 for the analysis and display of the results. Functional brain networks were computed for the theta band (4–7 Hz), alpha band (8–12 Hz), and beta band (13–30 Hz). After deriving the functional brain network, we analyzed its properties using graph theory to quantify its small-world characteristics. Specifically, we computed small-world metrics such as the clustering coefficient (CC), characteristic path length (L), betweenness centrality (BC), and global, local and nodal efficiency (Eff_{glob}, Eff_{loc}, Eff_{nod}). The betweenness centrality in EEG network analysis measured how pivotal a specific electrode or brain region was at connecting other regions by assessing its role as a bridge for information flow along the shortest paths within the network. Efficiency metrics in EEG network analysis encompass global efficiency, which evaluates the network-wide information flow and local efficiency, focusing on nearby node interactions and nodal efficiency while appraising the individual node's information transfer proficiency within the network. The clustering coefficient CC measures the level of local clustering or connectivity in the network, while L evaluates its overall routing efficiency [16].

3. Results

In the following diagrams, the evolution of the metrics (Eff_{nod}, Eff_{loc}, Eff_{glob}, CC, BC, and L) within the 1 h driving simulation is depicted for each frequency band, namely, theta alpha and beta bands (Figure 1), (Table 1). The first 5 min and last 5 min of the driving sessions were excluded from the analysis to avoid the inclusion of unrelated information.

Table 1. The values of the LSM slope for each metric during the whole driving task duration.

	L	*CC*	*BC*	Eff_{glob}	Eff_{loc}	Eff_{nod}
theta	0.0254	−0.0183	0.0061	−0.0265	−0.0205	−0.0265
alpha	−0.0288	0.0197	0.0077	0.0300	0.0235	0.0300
beta	−0.0157	0.0217	−0.008	0.0275	0.0281	0.0275

Namely, in the theta band, Eff_{nod}, Eff_{loc}, Eff_{glob} and CC decrease from the first to the last 5 min window, whereas BC and L increase within the same timeframe. Measures of efficiency, as well as clustering coefficient values depict a decrement in the early stage of the driving stimulation and a further decrement after the first half of it. As far as BC is concerned, it showed a stabilized pattern until the 15th to 16th window, when it started to decrease. On the other hand, L increased, at the early stage of the driving simulation and at the end of the experiment, tended to have a further increment.

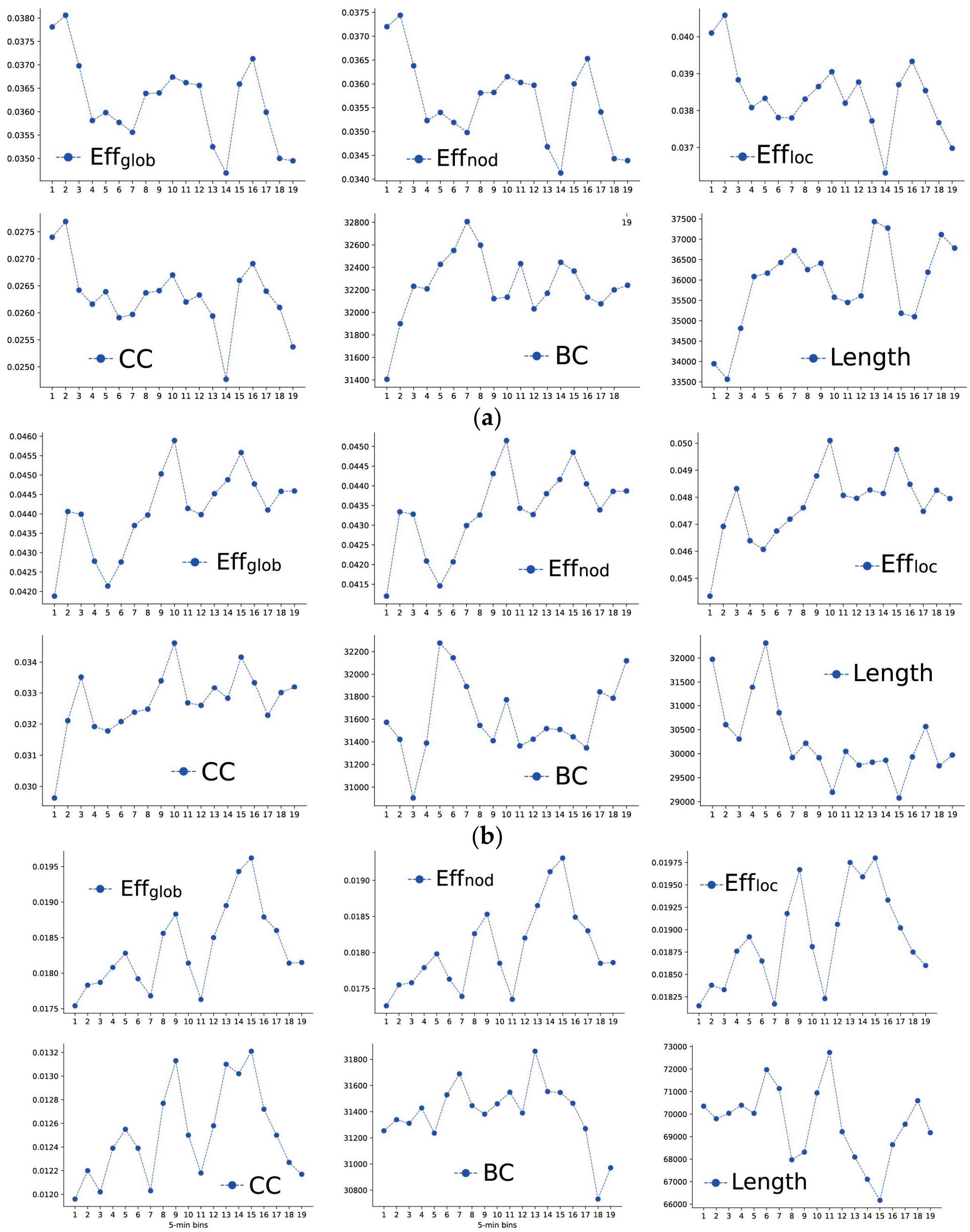

Figure 1. Evolution of small-world metrics during 19 windows of 5 min with a 50% overlap in: (**a**) Theta (**b**) Alpha and (**c**) Beta bands.

Alpha band measures of efficiency and CC increased from the beginning of the driving stimulation and remained rather stable for the rest of its duration. Betweenness centrality also increased, reaching a peak at an early stage of the driving before stabilizing at lower values and showing an increase again at the end of the experiment. Regarding the shortest path length, it showed a decrement in the first half of driving and remained stable until the end. In the theta band, Eff_{nod}, Eff_{loc}, Eff_{glob}, and C, comparing the first to the last 5 min window, showed decremental behavior, whereas BC and L increased within the same time frame. Concerning the measures of efficiency and CC, we could observe that there was a significant decrease in the first minutes of the driving simulation and showed a stabilized pattern until the 12th window, when unstable behavior started to conclude at an overall decrease in the last minutes of the experiment. As far as BC is concerned, a notable increase was performed in the first minutes of the simulation and afterward follows a rather stable pattern. On the other hand, L showed an almost constant increase from the early stage of the simulation, namely from the 4th window before reaching the highest point in the 17th window. For the beta band, the overall behavior of measures of efficiency and CC was slightly incremental, although their pattern was unstable throughout the whole driving period. Furthermore, BC also decreased in the end, although it was stable until the last time frame of the driving simulation. The average shortest path length was overall almost stable, although it was rather unstable for most of the time frames.

In order to compute the fitting line for the patterns of metrics, we used the method of least squares (LSM) in each of the frequency bands we examined above. The values of these slopes for the metrics' best-fitting lines are outlined in Table 1 for each of the examined frequency bands (theta, alpha, beta). To leverage the value of our results, we performed normalization (between 0 and 1) for all metrics' values, comparing them in a more concise and accurate manner.

It was observed that the most significant alterations in the metrics slopes were present in the alpha band. In the following diagrams (Figure 2), L and Eff_{glob} values are depicted, and the least square method fitting line is drawn, showing their pattern of alterations within the whole driving period.

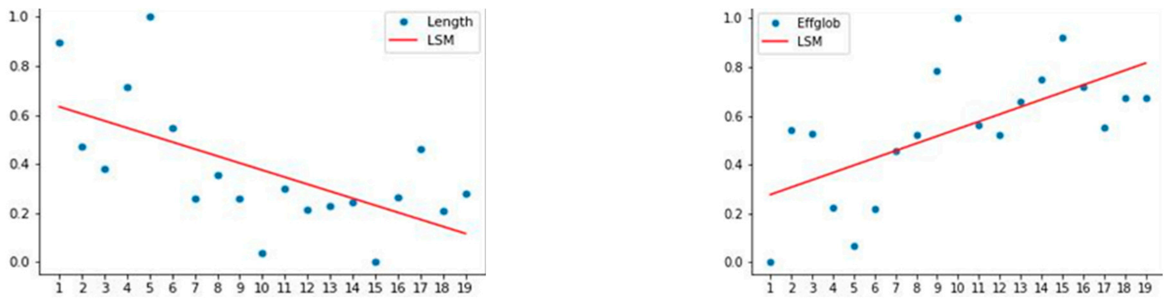

(**a**) (**b**)

Figure 2. Presentation of metrics during 19 windows of 5 min with a 50% overlap and the LSM fitting line in the alpha band for (**a**) Path length and (**b**) Global efficiency.

The next step in our analysis was to compute the correlation between all the metrics that were examined (Figure 3). The most significant correlation was observed between CC and Eff_{loc} (corr = 0.98) in all frequency bands and between CC and the other efficiency measures ranging from 0.89 to 0.93. Also, the Shortest Average Path Length was significantly and negatively correlated with all the measures of the efficiency and clustering coefficient ranging from −0.89 to −0.95. The only small-world metric that was not correlated with the rest of the metrics was BC.

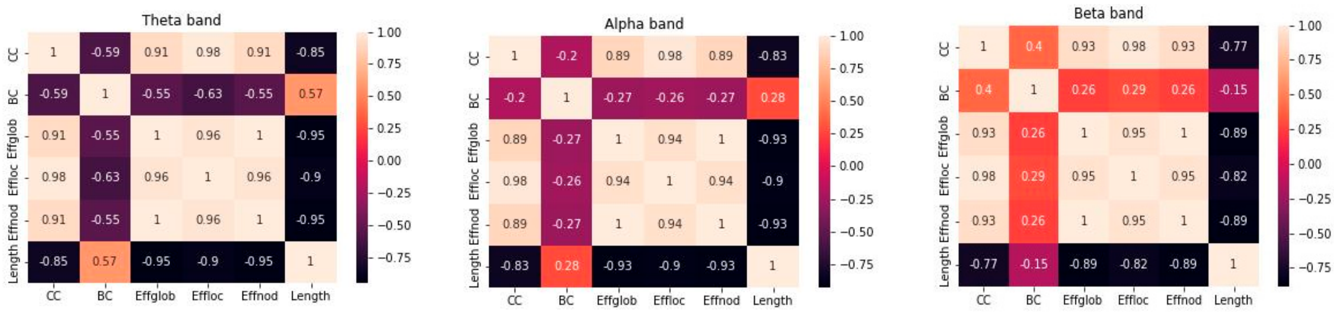

(**a**) (**b**) (**c**)

Figure 3. Correlation of small-world metrics during the whole driving task for: (**a**) Theta; (**b**) Alpha; and (**c**) Beta bands.

4. Discussion

The main results of this study are summarized as follows: From the first to the last 5 min bin, (1) Eff_{nod}, Eff_{loc}, Eff_{glob}, and CC in the beta band decreased significantly, whereas BC and L increased, and (2), in the alpha band, all of the metrics increased. (3) In the theta band, all measures of efficiency together with CC were overall decreased, while BC and L increased significantly. (4) It can be observed that CC and Eff_{loc} are highly correlated.

In this regard, the alpha band can be distinguished as the band with the most significant changes in the metric's time evolution, as these slopes showed the highest variations compared to the theta and beta bands. Our results are in line with the results of many other studies, where the alpha band is considered significant within many driving fatigue studies. Furthermore, it can be observed that CC and Eff_{loc} are highly correlated. In terms of the small-world metrics efficiency and cluster coefficient, a high correlation suggests a strong relationship between the local and global processing of information in the brain. In other words, brain regions that are highly interconnected with each other tend to be well-connected with distant brain regions. This is consistent with the notion of a small-world network, where the brain is able to balance local processing and the global integration of information.

Author Contributions: Conceptualization, Y.S. and G.N.D.; methodology, O.G., I.K. and G.N.D.; software, O.G. and G.N.D.; formal analysis, I.K.; investigation, Y.S. and I.K.; resources, Y.S. and G.K.M.; writing—original draft preparation, O.G.; writing—review and editing, I.K. and G.K.M.; visualization, G.N.D. and Y.S.; supervision, D.D.K.; project administration, Y.S., G.K.M. and D.D.K. All authors have read and agreed to the published version of the manuscript.

Funding: This research received no external funding.

Institutional Review Board Statement: The study was conducted in accordance with the Declaration of Helsinki and approved by the Institutional Review Board of NUS (B-15-169).

Informed Consent Statement: Informed consent was obtained from all subjects involved in this study.

Data Availability Statement: The data presented in this study are available on request. The data are not publicly available due to privacy reasons.

Acknowledgments: The authors want to thank Anastasios Bezerianos for his valuable support and guidance in the experimental design, data collection and analysis of this work.

Conflicts of Interest: The authors declare no conflict of interest.

References

1. Organização Mundial da Saúde. *Global Status Report on Road Safety 2018 Summary*; World Health Organization: Geneva, Switzerland, 2018; p. 20.
2. Bener, A.; Yildirim, E.; Özkan, T.; Lajunen, T. Driver sleepiness, fatigue, careless behavior and risk of motor vehicle crash and injury: Population based case and control study. *J. Traffic Transp. Eng. (Engl. Ed.)* **2017**, *4*, 496–502.
3. Van Cutsem, J.; Marcora, S.; De Pauw, K.; Bailey, S.; Meeusen, R.; Roelands, B. The Effects of Mental Fatigue on Physical Performance: A Systematic Review. *Sport. Med.* **2017**, *47*, 1569–1588. [CrossRef] [PubMed]
4. Monteiro, T.G.; Skourup, C.; Zhang, H. Using EEG for Mental Fatigue Assessment: A Comprehensive Look into the Current State of the Art. *IEEE Trans. Hum.-Mach. Syst.* **2019**, *49*, 599–610. [CrossRef]
5. Qi, P.; Ru, H.; Gao, L.; Zhang, X.; Zhou, T.; Tian, Y.; Thakor, N.; Bezerianos, A.; Li, J.; Sun, Y. Neural Mechanisms of Mental Fatigue Revisited: New Insights from the Brain Connectome. *Engineering* **2019**, *5*, 276–286. [CrossRef]
6. Zorzos, I.; Kakkos, I.; Miloulis, S.T.; Anastasiou, A.; Ventouras, E.M.; Matsopoulos, G.K. Applying Neural Networks with Time-Frequency Features for the Detection of Mental Fatigue. *Appl. Sci.* **2023**, *13*, 1512. [CrossRef]
7. Dimitrakopoulos, G.N.; Kakkos, I.; Vrahatis, A.G.; Sgarbas, K.; Li, J.; Sun, Y.; Bezerianos, A. Driving mental fatigue classification based on brain functional connectivity. *Commun. Comput. Inf. Sci.* **2017**, *744*, 465–474.
8. Dimitrakopoulos, G.N.; Kakkos, I.; Anastasiou, A.; Bezerianos, A.; Sun, Y.; Matsopoulos, G.K. Cognitive Reorganization Due to Mental Workload: A Functional Connectivity Analysis Based on Working Memory Paradigms. *Appl. Sci.* **2023**, *13*, 2129. [CrossRef]
9. Cao, J.; Zhao, Y.; Shan, X.; Wei, H.L.; Guo, Y.; Chen, L.; Erkoyuncu, J.A.; Sarrigiannis, P.G. Brain functional and effective connectivity based on electroencephalography recordings: A review. *Hum. Brain Mapp.* **2022**, *43*, 860–879. [CrossRef]

10. Kakkos, I.; Dimitrakopoulos, G.N.; Sun, Y.; Yuan, J.; Matsopoulos, G.K.; Bezerianos, A.; Sun, Y. EEG Fingerprints of Task-Independent Mental Workload Discrimination. *IEEE J. Biomed. Health Inform.* **2021**, *25*, 3824–3833. [CrossRef] [PubMed]
11. Sun, Y.; Lim, J.; Meng, J.; Kwok, K.; Thakor, N.; Bezerianos, A. Discriminative analysis of brain functional connectivity patterns for mental fatigue classification. *Ann. Biomed. Eng.* **2014**, *42*, 2084–2094. [CrossRef] [PubMed]
12. Dimitrakopoulos, G.N.; Kakkos, I.; Thakor, N.V.; Bezerianos, A.; Sun, Y. A mental fatigue index based on regression using mulitband EEG features with application in simulated driving. In Proceedings of the 2017 39th Annual International Conference of the IEEE Engineering in Medicine and Biology Society (EMBC), Jeju, Republic of Korea, 11–15 July 2017; pp. 3220–3223.
13. Stam, C.J.; Nolte, G.; Daffertshofer, A. Phase lag index: Assessment of functional connectivity from multi channel EEG and MEG with diminished bias from common sources. *Hum. Brain Mapp.* **2007**, *28*, 1178–1193. [CrossRef] [PubMed]
14. Smith, K.; Abásolo, D.; Escudero, J. Accounting for the complex hierarchical topology of EEG phase-based functional connectivity in network binarisation. *PLoS ONE* **2017**, *12*, e0186164. [CrossRef] [PubMed]
15. Goswami, S.; Murthy, C.A.; Das, A.K. Sparsity measure of a network graph: Gini index. *Inf. Sci.* **2018**, *462*, 16–39. [CrossRef]
16. Bassett, D.S.; Bullmore, E. Small-World Brain Networks. *Neurosci.* **2016**, *12*, 512–524. [CrossRef] [PubMed]